# Controlling the morphology and optical properties of self-assembled InAsSb/InGaAs/InP nanostructures via Sb exposure

W. Lei, H. H. Tan, and C. Jagadish

Citation: Appl. Phys. Lett. **99**, 193110 (2011); doi: 10.1063/1.3659695
View online: http://dx.doi.org/10.1063/1.3659695
View Table of Contents: http://apl.aip.org/resource/1/APPLAB/v99/i19
Published by the American Institute of Physics.

# Controlling the morphology and optical properties of self-assembled InAsSb/InGaAs/InP nanostructures *via* Sb exposure

W. Lei,[a] H. H. Tan, and C. Jagadish
*Department of Electronic Materials Engineering, Research School of Physics and Engineering, The Australian National University, Canberra ACT 0200, Australia*

(Received 13 October 2011; accepted 18 October 2011; published online 11 November 2011)

Engineering the surface energy, interface energy, and elastic strain energy in the system *via* Sb exposure is used to realize the control on the morphology and optical properties of self-assembled InP-based InAsSb/InGaAs nanostructures. By flowing trimethylantimony precursor over the surface of InGaAs buffer layer before the growth of InAsSb nanostructures, the surface/interface energy in the system is reduced, while the strain energy in the system is enhanced, which lead to a shape transition from dot to dash, and to wire for the InAsSb nanostructures. As a result of their morphology changes, the InAsSb nanostructures show different polarization characteristics in their photoluminescence emission. © *2011 American Institute of Physics*. [doi:10.1063/1.3659695]

Surface energy, interface energy, and elastic strain energy play a critical role in the epitaxy of self-assembled semiconductor nanostructures like quantum dots (QDs), quantum dashes (QDashes), and quantum wires (QWRs), which have great potential applications in optoelectronic devices.[1] The well-established Stranski–Krastanow (S-K) growth of these nanostructures is based on the competition between surface energy, including interface energy and elastic strain energy in the system.[1,2] By engineering the surface/interface energy, and elastic strain energy in the system, one can control the morphology of nanostructures and thus their resultant physical properties.[2] However, the widely used approaches to control their morphology and their physical properties are almost all based on changing the growth parameters during the growth of these nanostructures, like growth temperature and growth rate.[1,3,4] Little is known about the approach *via* the surface/interface energy and strain energy engineering.[2]

It is the purpose of this work to demonstrate the feasibility of surface/interface energy and strain energy approaches to control the morphology and optical properties of self-organized InAsSb/InGaAs/InP nanostructures, which have important applications in mid-infrared emitters.[5] By using antimony (Sb) exposure to modify the surface/interface energy, and elastic strain energy in the system, the morphology of InAsSb nanostructures can be well controlled, and various nanostructure shapes like dot, dash, and wire can be achieved. Their optical properties also correspond well with the shape changes caused by Sb exposure.

The InAsSb nanostructures were grown on semi-insulating InP (001) substrates in a horizontal flow Metal-Organic Chemical Vapour Deposition reactor (AIX200/4) at a pressure of 180 mbar. Trimethylindium (TMIn), trimethylgallium (TMGa), trimethylantimony (TMSb), $PH_3$, and $AsH_3$ were used as the precursors and ultra-high purity $H_2$ as the carrier gas. The InAsSb/InGaAs nanostructures were grown using the following layer sequence: first, a 50 nm InP layer and 100 nm $In_{0.53}Ga_{0.47}As$ matrix layer were deposited at 650 °C, then the temperature was dropped to 480 °C to grow 4 monolayers (MLs) of $InAs_{0.5}Sb_{0.5}$ nanostructure layer which was immediately capped with 5 nm $In_{0.53}Ga_{0.47}As$ without any growth interruption. After that the temperature was ramped up to 650 °C and a 100 nm, $In_{0.53}Ga_{0.47}As$ spacer layer was deposited. The same steps were followed to grow a top layer of $InAs_{0.5}Sb_{0.5}$ nanostructures for atomic force microscopy (AFM) measurements. To investigate the influence of surface energy and elastic strain energy on the S-K growth of InAsSb nanostructures, just prior to InAsSb deposition and at 480 °C, antimony was exposed onto the sample surface for various times ($t_{Sb}$), namely 0, 4, 8, and 15 s (s) for sample A, B, C, and D, respectively, by flowing TMSb at $1 \times 10^{-4}$ mol/min with all other sources removed from the reactor. During the growth of InAsSb layers TMIn, TMSb and $AsH_3$ sources were introduced simultaneously. The morphology of the top InAsSb nanostructures was characterized by using AFM in tapping mode. Raman scattering measurements were performed in backscattering geometry at room temperature with a Renishaw 2000 confocal micro-Raman system, where $z(x', x'+y')\bar{z}$ polarization configuration ($x \| [100]$, $y \| [010]$, $z \| [001]$, $x' \| [110]$, and $\| y' \| [1-10]$) was used. The samples were excited by the 632.8 nm line of a He-Ne laser to a 2 $\mu$m spot on the surface with an excitation power of 4 mW. Photoluminescence (PL) measurements were carried out under excitation by a 637 nm laser diode. The luminescence signal was collected by a liquid nitrogen-cooled extended InGaAs photodetector through a 0.5 m monochromator.

Figure 1 shows the morphology evolution of InAsSb nanostructures with increasing $t_{Sb}$. Clearly, InAsSb QDs are obtained without Sb exposure. However, with increasing $t_{Sb}$ dash and wire structures are formed instead of dot structures. The InAsSb nanostructures have an average height of ~1.3, 1.2, 1, and 0.9 nm, lateral width (along the [110] direction) of ~31, 23, 20, and 15 nm, length (along the [1-10] direction) of ~40, 70, 84, and 140 nm for samples A, B, C, and D, respectively. With increasing $t_{Sb}$, the height and lateral width of InAsSb nanostructures decreases to some extent, while their length increases significantly. This morphology change

[a]Electronic mail: wen.lei@anu.edu.au.

 

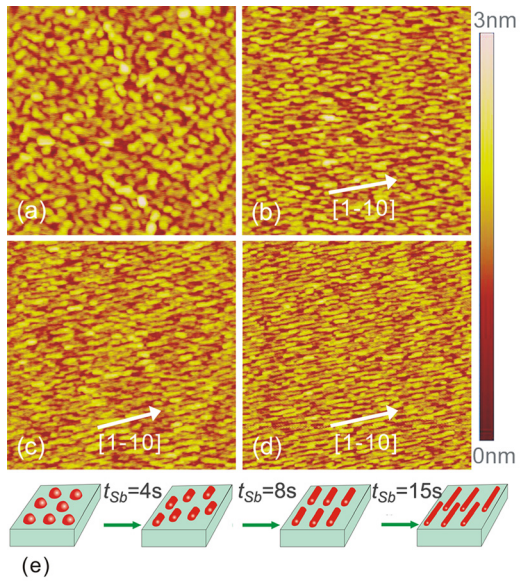


FIG. 1. (Color online) AFM images of samples A (a), B (b), C (c) and D (d), and schematic diagram of the island's shape evolution with increasing the $t_{Sb}$ from 0 to 15 s (e). Scan size of (a), (b), (c), and (d) is 1 $\mu m^2$.

is quite unexpected from what is normally reported. As for the Sb-mediated growth of QDs, two resultant effects on the subsequent nucleation of QDs may be observed depending on the amount of Sb used. One is that when using a small amount of antimony rougher surfaces with a higher step density will be formed which then provide many nucleation sites for the growth of three-dimensional (3D) islands, leading to the formation of high density QDs.[6–9] However, AFM study (images not shown here) on bare $In_{0.53}Ga_{0.47}As$ layers shows that the surface roughness doesn't increase after Sb exposure for 4, 8 and 15 s with the same TMSb flow and at 480 °C. The other is that when using a large amount of antimony some Sb atoms will be accumulated on the surface. This will significantly reduce the diffusion of the group III atoms and suppress the growth of 3D islands, resulting in the growth of quantum well (QW) structures.[10,11] This effect is different from what we observed here.

To interpret the unusual experimental phenomena here, the theoretical approach of Tersoff and Tromp[2] is adopted by taking into account the change of surface/interface energy and elastic strain energy after Sb exposure. Generally, with sufficient diffusion of the adatoms, the island's shape is mainly determined by the thermodynamic equilibrium of the system. The shape change is governed by the island energy per unit volume

$$\frac{E}{V} = 2\Gamma\left(\frac{1}{s}+\frac{1}{l}\right) - 2ch\left[\frac{1}{s}ln\left(\frac{s}{\phi h}\right)+\frac{1}{l}ln\left(\frac{l}{\phi h}\right)\right], \quad (1)$$

where $s$, $l$, and $h$ are the island width, length, and height, $V = hsl$ is the island volume and $E$ the total energy. $\Gamma = \gamma_e \csc\theta - \gamma_s \cot\theta$, where $\theta$ is the angle between the island side facet and the substrate and $\gamma_e$ and $\gamma_s$ are the surface energies per unit area of the island edge facet and the substrate. $c = \sigma_b^2(1-\nu)/2\pi\mu$, where $\sigma_b$ is the bulk stress and $\nu$ and $\mu$ are the Poisson ratio and shear modulus of the substrate, respectively, and $\phi = e^{-3/2}\cot\theta$. The first term in

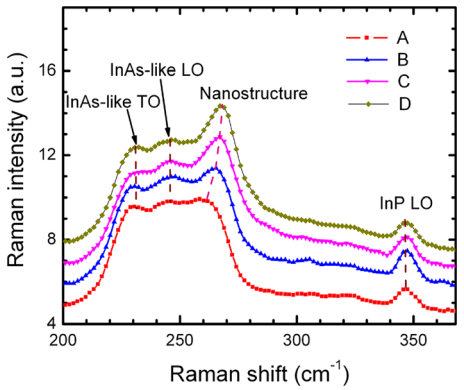


FIG. 2. (Color online) Raman spectra of sample A, B, C and D.

Eq. (1) is the surface plus interface energy in the presence of a wetting layer and the second term the elastic strain energy. For an island with a given volume and fixed height, minimization of the total energy with respect to the island width $s$ and length $l$ results in stable square shaped island with $s = l$ only for island sizes $s = l < e\alpha_0$, $\alpha_0 = e\phi h e^{\Gamma/ch}$. For larger islands with sizes beyond $e\alpha_0$, the stable shape is rectangular and the larger the difference between the island sizes grown and the critical size $e\alpha_0$, the larger the length/width ratios of the islands grown. Therefore, for an island with a given volume and fixed height, its shape can be controlled from dot to dash and to wire by changing the critical size $e\alpha_0$, which can be realized by engineering the surface/interface energy, and elastic strain energy in the system through Sb exposure. On the one hand, the Sb exposure onto InGaAs surface will significantly reduce the surface/interface energy in the system[10–12]; on the other hand, the Sb atoms exposed onto the InGaAs surface might be incorporated into the InAsSb layers deposited subsequently, leading to larger lattice mismatch (strain) between InAsSb layers and InGaAs layers. As discussed above, both the decrease of surface/interface energy and the increase of strain in the system will cause a smaller critical size $e\alpha_0$, leading to a shape transition from square to rectangular for the island. Furthermore, the smaller the critical size $e\alpha_0$, the larger the length/width ratio of the island grown. This is well confirmed by the size evolution of the grown islands here.

The model discussed above is based on the decrease of surface/interface energy and increase of strain in the system after Sb exposure. The role of Sb atoms to reduce surface/interface energy in the system has been widely reported (see Refs. 10–12), which leaves the study of strain in the system as the focus of this work. Figure 2 shows the Raman spectra obtained on samples A, B, C, and D. The Raman peak located around 261 ~ 268 $cm^{-1}$ can be determined to arise from the InAsSb nanostructures (261, 265, 267, and 268 $cm^{-1}$ for samples A, B, C, and D, respectively) due to the fact that its position shifts with increasing the $t_{Sb}$.[13–15] Generally, for a perfect heterostructure, both compressive strain (upward shift) and confinement effects (downward shift) play a dominant role in the observed phonon frequency shift ($\Delta\omega_{exp}$): ($\Delta\omega_{exp} = \Delta\omega_{strain} + \Delta\omega_c$).[16,17] When $t_{Sb}$ increases from 0 to 15 s, the island height decreases from 1.3 to 0.9 nm, suggesting a slight increase of phonon

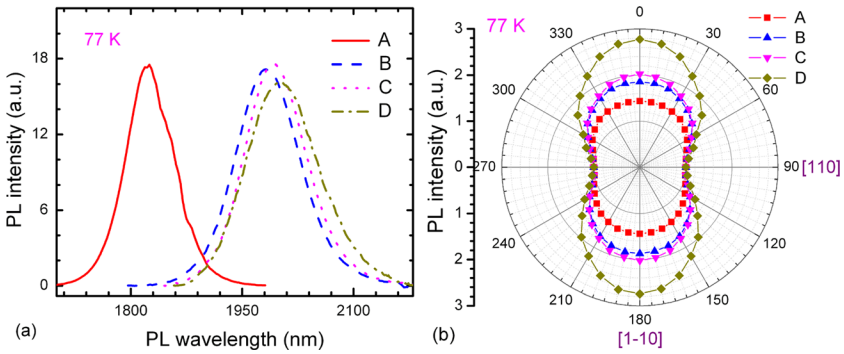


FIG. 3. (Color online) 77 K PL spectra (a) and 77 K polar scan of the polarized PL intensity (b) of sample A, B, C and D.

confinement effect in the islands and thus a small downward frequency shift (0.2 $cm^{-1}$ for $InAs_{0.5}Sb_{0.5}$ islands according to the modified spatial correlation model[18,19]). However, the phonon peak of InAsSb islands shows an upward frequency shift from 261 to 268 $cm^{-1}$ experimentally, indicating that with increasing $t_{Sb}$ from 0 to 15 s, the compressive strain in the InAsSb islands has increased significantly (the phonon frequency shift from 261 to 265, to 267, and to 268 $cm^{-1}$ corresponds to an increase of compressive strain from 4.8% to 6.0%, to 6.6%, and to 6.9% for InAsSb islands according to the model and parameters reported in Ref. 16, 17, and 20) and induced an upward frequency shift far surpassing the downward frequency shift caused by phonon confinement effect. This large increase of compressive strain with increasing $t_{Sb}$ is mainly caused by the incorporation of surface Sb atoms into InAsSb islands though the change of island geometry also has little influence

The InAsSb islands with different geometric shapes exhibit different optical polarization characteristics. Figure 3 shows the 77 K PL spectra and emission polarization features of samples A, B, C, and D. It is observed that the PL peak shifts from 1821 nm (A) to 1986 nm (B), to 1992 nm (C), and to 2000 nm (D) as $t_{Sb}$ increases from 0 to 15 s. The red-shift with increasing $t_{Sb}$ is mainly caused by the incorporation of surface Sb atoms into InAsSb layers. By assuming that the compressive strain in InAsSb islands is mainly caused by the lattice mismatch between InAsSb islands and InGaAs matrix, the average Sb composition (mole fraction) in InAsSb islands can be roughly estimated to be 22%, 39%, 47%, and 51% for sample A, B, C, and D, respectively, according to the average compressive strain deduced from the Raman measurements. It is reported that the band gap of $InAs_{1-x}Sb_x$ alloy has its minimum value when the Sb composition $x$ is around 50%.[5] So, the significant increase of average Sb composition in InAsSb islands with the increase of $t_{Sb}$ from 0 to 15 s results in a substantially reduced band gap and thus a net red-shift for their PL peak. Figure 3(b) shows the polar scan of PL intensity of the samples. Obviously, the optical anisotropy of the InAsSb island increases significantly as $t_{Sb}$ increases, which is mainly caused by their shape anisotropy despite strain having some influence.

In summary, the controlled fabrication and optical properties of InAsSb/InGaAs/InP nanostructures have been demonstrated *via* engineering surface/interface energy and elastic strain energy in the system. The Sb exposure onto the surface of InGaAs buffer layers before the island growth is used to modify the surface/interface energy and elastic strain energy in the system. With increasing the Sb exposure time, the surface/interface energy in the system is significantly reduced, while the elastic strain energy in the system is substantially increased due to the incorporation of surface Sb atoms into the subsequent growth of InAsSb islands. This induces an evolution of island shape from dot structure to wire structure. As a result of their different shape anisotropy, the InAsSb islands show different polarization characteristics for their PL emission, which provides a potential approach to make polarization selective devices.

Financial support from Australian Research Council is gratefully acknowledged.

[1]For a review, see D. Bimberg, M. Grundmann, and N. N. Ledentsov, *Quantum Dot Heterostructures* (Wiley, New York, 1999).
[2]J. Tersoff and R. M. Tromp, Phys. Rev. Lett. **70**, 2782 (1993).
[3]W. Q. Ma, R. Nötzel, H. P. Schönherr, and K. H. Ploog, Appl. Phys. Lett. **79**, 4219 (2001).
[4]V. G. Dubrovskii, G. E. Cirlin, Y. G. Musikhin, Y. B. Samsonenko, A. A. Tonkikh, N. K. Polyakov, V. A. Egorov, A. F. Tsatsul'nikov, N. A. Krizhanovskaya, V. M. Ustinov, *et al*., J. Cryst. Growth **267**, 47 (2004).
[5]C. Cornet, F. Doré, A. Ballestar, J. Even, N. Bertru, A. Le Corre, and S. Loualiche, J. Appl. Phys. **98**, 126105 (2005).
[6]N. Kakuda, S. Tsukamoto, A. Ishii, K. Fujiwara, T. Ebisuzaki, K. Yamaguchi, and Y. Arakawa, Microelectronics J. **38**, 620 (2007).
[7]D. Guimard, M. Nishioka, S. Tsukamoto, and Y. Arakawa, Appl. Phys. Lett. **89**, 183124 (2006).
[8]P. Aivaliotis, L. R. Wilson, E. A. Zibik, J. W. Cockburn, M. J. Steer, and H. Y. Liu, Appl. Phys. Lett. **91**, 013503 (2007).
[9]N. Kakuda, T. Yoshida, and K. Yamaguchi, Appl. Surf. Sci. **254**, 8050 (2008).
[10]B. Voigtlander, A. Zinner, T. Weber, and H. P. Bonzel, Phys. Rev. B **51**, 7583 (1995).
[11]T. Matsuura, T. Miyamoto, T. Kageyama, M. Ohta, Y. Matsui, T. Furuhata, and F. Koyama, Jpn. J. Appl. Phys. **43**, L605 (2004).
[12]A. Portavoce, I. Berbezier, and A. Ronda, Phys. Rev. B **69**, 155416 (2004).
[13]L. Artús, R. Cuscó, S. Hernández, A. Patanè, A. Polimeni, M. Henini, and L. Eaves, Appl. Phys. Lett. **77**, 3556 (2000).
[14]W. Lei, Y. H. Chen, B. Xu, X. L. Ye, Y. P. Zeng, and Z. G. Wang, Nanotechnology **16**, 1974 (2005).
[15]W. Lei, H. H. Tan, C. Jagadish, Q. J. Ren, J. Lu, and Z. H. Chen, Appl. Phys. Lett. **97**, 223108 (2010).
[16]I. Rasnik, M. J. S. P. Brasil, F. Cerdeira, C. A. C. Mendonca, and M. A. Cotta, J. Appl. Phys. **87**, 1165 (2000).
[17]B. Jusserand and M. Cardona in *Light Scattering in Solids V: Topics in Applied Physics*, edited by M. Cardona and G. Güntherodt (Springer, Heidelburg, 1989), Vol. 66.
[18]H. Richter, Z. P. Wang, and L. Ley, Solid State Commun. **39**, 625 (1981).
[19]I. H. Campbell and P.M. Fauchet, Solid State Commun. **58**, 739 (1986).
[20]R. Carles, V. Saint-Cricq, J. B. Renucci, M. A. Renucci, and A. Zwick, Phys. Rev. B **22**, 4804 (1980).